NANO-MICRO LETTERS ARTICLE
www.nmletters.org

Electrochemical Generation of Cubic Shaped Nano Zn_2SnO_4 Photocatalysts

Chandrappa K. Govindappa[1,2,*], Venkatesha T. Venkatarangaiah[2], Sharifah B. Abd Hamid[1]

(Received 7 March 2013; accepted 24 April 2013; published online 10 May 2013)

Abstract: In this contribution, an efficient and simple two-step hybrid electrochemical-thermal route was developed for the synthesis of cubic shaped Zn_2SnO_4 (ZTO) nanoparticles using aqueous sodium bicarbonate ($NaHCO_3$) and sodium stannate (Na_2SnO_3) electrolyte. The sacrificial Zn was used as anode and cathode in an undivided cell under galvanostatic mode at room temperature. The bath concentration and current density were respectively varied from 30 to 120 mmol and 0.05 to 1.5 A/dm^2. The electrochemically generated precursor was calcined for an hour at different range of temperature from 60 to 600℃. The crystallite sizes in the range of 24-53 nm were calculated based on Debye-Scherrer equation. Scanning electron microscope and transmission electron microscopy results reveal that all the particles have cubic morphology with diameter of 40-50 nm. The as-prepared ZTO samples showed higher catalytic activity towards the degradation of methylene blue (MB) dye, and 90% degradation was found for the sample calcined at 600℃, which is greater than that of commercial TiO_2-P25 photocatalysts. The photodegradation efficiency of ZTO samples was found to be a function of exposure time and the dye solution pH value. These results indicate that the ZTO nanoparticles may be employed to remove dyes from wastewater.

Keywords: Electrochemistry; Zn_2SnO_4; Photocatalyst; Cubic; Nanoparticle

Citation: Chandrappa K. Govindappa, Venkatesha T. Venkatarangaiah and Sharifah B. Abd Hamid, "Electrochemical Generation of Cubic Shaped Nano Zn_2SnO_4 Photocatalysts", Nano-Micro Lett. 5(2), 101-110 (2013). http://dx.doi.org/10.5101/nml.v5i2.p101-110

Introduction

Metal metal-oxide nanostructured materials have been attracted much attention due to their prominent properties and potential applications in heterogeneous catalysis, optoelectronics, metallurgy, thin film coating, fine ceramic composites and photocatalysts [1]. Semiconductor oxide materials such as ZnO, CuO, TiO_2, Al_2O_3, SnO_2, ZrO_2 and WO_3 are attractive photocatalysts because they are not only environmentally sustainable but also high catalytic efficiency in degradation of various environmental pollutants such as pesticides, detergents, dyes and volatile organic compounds [2-5]. Ternary semiconductor oxides Zn_2SnO_4 (ZTO) is known for owning high-electron mobility, high-electrical conductivity, low visible absorption and attractive optical properties, which makes it suitable for applications in solar cell [6], gas sensor (detecting humidity and various combustible gases) [7,8], photoluminescence, negative electrode of Li-ion battery [9,10] and photocatalysis (degrading organic pollutants) [11-13].

ZTO (Zinc stannate) is a transparent semiconducting oxide material and has attracted considerable interest for its high photocatalytic activity. The decomposition reactions of benzene and water soluble dyes using ZTO as a photocatalyst were reported [11,12,14,15]. In early 2000s, there were some reports on synthesis and photocatalytic properties of ZTO nanostructures. Lou *et*

[1]Nanotechnology & Catalysis (NANOCAT) research centre, IPS Building, University of Malaya, 50603, Kuala Lumpur, Malaysia
[2]Department of Chemistry, Jnana Sahyadri, Kuvempu University, Shankaraghatta-577451, Karnataka, India
*Corresponding author. E-mail: chandukodi@yahoo.co.in

al. used one-step hydrothermal method to prepare ZTO nanocrystal at 200℃ and discussed their photocatalytic propertiers on reactive dyes K-NR, B-RN and B-GFF [11]. Cun *et al.* have used coprecipitation method for the preparation of nano-sized ZTO and the research of their photocatalytic activities to benzene [12]. Foletto *et al.* have synthesized ZTO by hydrothermal method at 200℃ for 12 hr and investigated their photocatalytic activities on leather dye [14]. Several other literatures reporting synthesis and properties of ZTO nanostructures were also published ever since [15-22].

Large number of methods have been developed for the preparation of ZTO, such as thermal evaporation [23,24], high temperature calcination [12,25], sol-gel synthesis [26,27], mechanical grinding [28] and hydrothermal reaction [6,10,11,18,29-31]. Among these methods, the electrochemical method has aroused a considerable interest in the synthesis of nanosized metal metal-oxide powder and films because of its simplicity, low temperature operation process and viability of commercial production. This method is also a simpler and more effective way to prepare well-crystallized ZTO with pure phase, which is difficultly obtained by high-temperature solid state reactions among the evaporated ZnO atmosphere, generally. On the contrary, the electrochemical preparations were usually performed in an aqueous solution using $NaHCO_3$ as mineralizer.

Increased human population has resulted in the development of large-scale industries such as textile and paper production, whose waste products cause a major environmental hazard to aquatic biota and humans due to their toxicity [32] and the tendency to cause eutrophication [2]. Detection and removal of these toxic chemicals is a major challenge with convention methods. Thus, there is an urgent need of eco-friendly technologies for the detection and removal of textile effluents from water. It has been shown that dyes can be easily adsorbed and catalyzed on oxide surfaces. However, to the best of our knowledge, there exist only a few reports [33-37] on the direct removal of commonly used industrial dyes. In the present investigation, we focus on the bulk synthesis of cubic shaped ZTO nanoparticles with a hybrid electrochemical-thermal route without using any template or surfactant at room temperature. The effects of electrolyte, current density and reaction media on the shape, size, chemical composition of the generated product, together with the production yield were investigated. FT-IR absorption spectra, SEM and TEM images and power XRD patterns of the products calcined at different temperatures were tested and discussed. It has been found that our method is a simple and feasible electrochemical route for the synthesis of ZTO nanoparticles on commercial scale. As well, the spectroscopic spectra and degradation ratio of commonly used textile dye (Methylene Blue; cationic) in aqueous solution with these ZTO nanoparticles were tested under different UV irradiation time, to characterize ZTO nanoparticles' photocatalytic properties. The optimum conditions for generation of ZTO nanoparticles were also proposed.

Experimental Procedure

Materials

High purity Zinc metal plate (99.99%), sodium bicarbonate (AR grade: 99.5%), sodium stannate (AR grade: 98.5 %) purchased from Sisco Research laboratories, Mumbai and Methylene Blue (MB) from S. D. Fine Chemicals Ltd., India, were used as received. Millipore water (specific resistance, 15 MΩ cm at 25℃, Millipore Elix 3 water purification system, France) was used to prepare the electrolyte solution.

Synthesis of ZTO nanoparticles

ZTO nanoparticles were synthesized using a standard electrochemical technique mentioned in ref [38]. Prior to electrolysis, the Zn plates were activated by immersing in dilute HCl (1 M) for 30 sec followed by washing with Millipore water. The electrolyte was a 400 ml solution containing 30 mM (1.008 gm) $NaHCO_3$ and 10 mM Sodium stannate. It was injected in a rectangular undivided cell ($5.0 \times 6.0 \times 0.8$ cm^3) where Zn plates were used as both cathode and anode. The electrolysis was carried out for about one hour under galvanostatic conditions, the constant current was supplied by a DC power supply (model PS 618 potentiostat/galvanostat 302/2 A supplied by Chem link, Mumbai) with constant stirring at 600 rpm. The schematic diagram of electrolysis process is shown in Fig. 1. The pH of the electrolyte was recorded before and after the electrolysis. A white precipitate was formed and filtered (by whattman filter paper No.41) to isolated from the solution. The final product of solution follows the reaction mechanism,

$$Zn \rightarrow Zn^{2+} + 2e^- \quad \text{(on anode)} \tag{1}$$

$$2H^+ + 2e^- \rightarrow H_2 \uparrow \quad \text{(on cathode)} \tag{2}$$

$$2NaHCO_3 + 2H_2O \rightarrow 2Na^+ + 4OH^- + 2CO_2 \uparrow + H_2 \uparrow \quad \text{(in electrolyte solution)} \tag{3}$$

$$Na_2SnO_3 + 3H_2O \rightarrow Sn^{4+} + 2Na^+ + 6OH^- \quad \text{(in electrolyte solution)} \tag{4}$$

$$Zn^{2+} + Sn^{4+} + 6OH^- \rightarrow ZnSn(OH)_6 \downarrow \quad \text{(precipitate)} \tag{5}$$

$$Zn^{2+} + 4OH^- \rightarrow Zn(OH)_4^{2-} \quad \text{(soluble complex)} \tag{6}$$

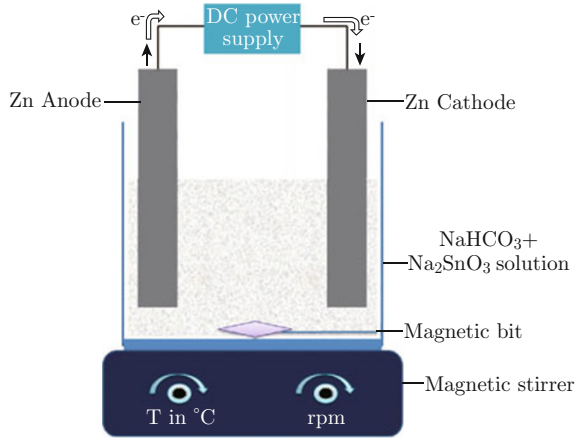

Fig. 1 Schematic diagram of electrolysis process.

The resulting wet precipitate was dried at 60℃ in hot air oven for 1 hr and then it was calcined at 300℃ or 600℃ for 1 hr. The calcined product follows the reaction,

$$ZnSn(OH)_6 + Zn(OH)_4^{2-} \rightarrow Zn_2SnO_4 \downarrow + 4H_2O + 2OH^- \quad (7)$$

The same procedure was also repeated using 60 and 120 mM of $NaHCO_3$ and 0.01M Na_2SnO_3.

Characterization

The morphology, structure, crystallite size and compositional analysis of the nanoparticles were performed using powder X-ray diffraction (XRD), transmission and scanning electron microscopy and FT-IR spectroscopy. Morphology and compositional analysis were carried out in a scanning electron microscope (SEM, Philips XL 30) in the voltage range of 200-300 kV. Transmission electron microscope (TEM, JEOL 2000 FX-II) images of selected samples were recorded with an acceleration voltage of 200 kV. A 2 µl of ZTO-ethanol solution was dropped on a Cu grid with a carbon-reinforced plastic film. Powder X-ray diffraction (XRD) patterns were tested for all the samples using PANalytical X'pert Pro powder diffractometer with Cu-K_α radiation, (λ_{Cu}=1.5418 Å) working at 30 mA and 40 kV. The XRD patterns were recorded in the 2θ range from 10° to 80° at a scanning rate of 1°/min. Fourier transform infrared spectra (FT-IR) were obtained on KBr pellets at ambient temperature using a Bruker FT-IR spectrometer (TENSOR 27). The average crystallite sizes were calculated by using the Debye-Scherrer equation $D = K\lambda/\beta\cos\theta$ [39], where D is the diameter of the crystallite size, K is the shape factor (the typical value is 0.9) λ is the wavelength of incident beam, β is the broadening of the diffraction peak measured in radians at half of its maximum intensity (FWHM) and θ is the Bragg's angle.

Photocatalytic degradation of MB dye in aqueous solution

Photocatalysis experiments were carried out with different sized (24, 35 and 53 nm) ZTO nanoparticles (0.1 g in 100 ml of dye solution) and Methylene blue (MB) dye solution (10 ppm) in Millipore water. The photochemical reactor used in this study was made of a Pyrex glass jacketed quartz tube. A high pressure mercury vapor lamp (HPML) of 125 W (Philips, India) was placed inside the jacketed quartz tube. To avoid fluctuations of the input light intensity, a supply ballast and capacitor were connected in series with the lamp. Water was circulated through the annulus of the quartz tube to avoid overheating of the solution. Synthesized ZTO nanoparticles of varying sizes were added to 100 ml dye solution (10 ppm), with continuous stir for 2 hr for homogeneity. 100 ml of the solution (ZTO and MB) was taken in the beaker under continuous stir to ensure the uniform suspension of the catalyst. The lamp radiated predominantly at 365 nm, corresponding to photon energy of 3.4 eV and photon flux of 5.8×10^{-6} mol of photons sec^{-1}. Aliquots were collected from the reaction beaker at regular time intervals, and the concentration of dye in solution and degradation ratio was plotted as a function of time by monitoring the changes of the λ_{max} line intensity with time.

Results and discussion

X-ray diffraction to study ZTO

The phase purity and crystalline structure of all synthesized powders were investigated using powder X-ray diffraction technique. The powder XRD patterns for the as-prepared and calcined compounds prepared under the electrolytic concentration of 30 mM $NaHCO_3$, 10 mM Na_2SnO_3 and the current density of 1 A/dm^2 were shown in Fig. 2. It can be seen from Fig. 2(a) that the eleven peaks appeared at 19.8°, 22.9°, 27.9°, 31.9°, 32.6°, 38.6°, 40.3°, 46.8°, 47.6°, 52.6° and 58.0° correspond to the characteristic peaks of zinc tin hydroxide [Zn·Sn$(OH)_6$] phase, (recorded by standard JCPDS file no. 74-1825). Also, the other six peaks appeared at 34.4°, 36.2°, 56.6°, 63.1°, 68.2° and 73.2° correspond to the characteristic peaks of Zn_2SnO_4. The XRD patterns for the calcined samples at 300℃ for 1 hr (Fig. 2(b)) could be completely indexed to cubic phase (JCPDS file No. 24-1470). Similar observation was also made by M. J. Kim et al. [21]. The powder XRD pattern for the sample calcined at 600℃ is presented in Fig. 2(c). Figure 2(b-c) reveals that an increasing calcination temperature from 300 to 600℃, made the characteristic Zn_2SnO_4 peaks sharper and the crystallanity increased. The crystallite size (d) was found to be 49 nm, estimated from the full width at half

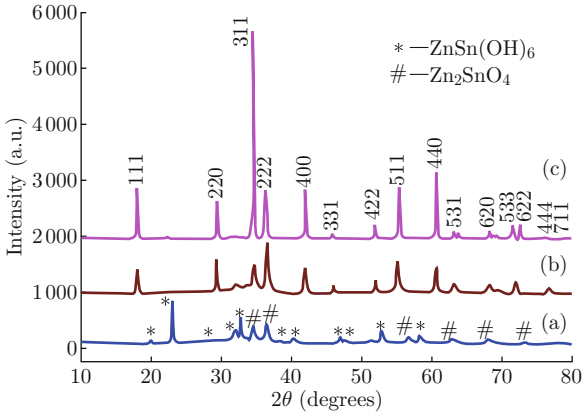

Fig. 2 XRD patterns of (a) ZTO precursor, (b) calcined at 300℃, and (c) calcined at 600℃.

maximum (w) of the dominant (311) peak at diffraction angle $2\theta \approx 34.4°$ using Debye Scherrer's equation. All the calcined powders of XRD patterns were indexed to the pure cubic structure with a lattice parameter of 8.657(6) Å and its space group: Fd-3m (227). They are matching with the standard JCPDS card No. 24-1470, indicating that the ZTO particles are crystalline with face centered cubic structure. From the XRD data, the average crystallite sizes were found to be 24, 35 and 53 nm, respectively. It clearly indicates that, the non crystalline Zn·Sn$(OH)_6$ phase were gradually converted to cubic crystalline phase of ZTO nanoparticles. No peaks related to other phases and impurities were found in XRD patterns of calcined compounds, implying the formation of pure ZTO nanoparticles and these particles are fcc Bravias lattice in nature.

Surface morphological studies

Scanning and transmission electron micrographs of as-prepared and calcined compounds of ZTO nanopowder are shown in Fig. 3. The as-prepared compound was synthesized from the bath with concentration of 30 mM $NaHCO_3$, 10 mM Na_2SnO_3 and the current density of 1 A/dm^2, and in sequence, it was calcined for 1 hr at 300℃ or 600℃. The SEM images of ZTO nanoparticles show different morphologies. Figure 3(a) presents the SEM image of the starting Zn·Sn$(OH)_6$ compound. It can be seen that the particles exhibit irregular, agglomerated small flower like structure, whereas calcined powder at 300℃ shows less randomly oriented cubic like morphology (Fig. 3(b)). The small flowers of the starting compound transformed to cubic like ZTO structures, starting at 300℃ and speeding up at 600℃. The as-prepared sample heated at 600℃ for 1 hr (Fig. 3(c)) produces uniformly oriented cubic structure due to the growth of ZTO particles. As the heat treatment temperature increases, the particles tend to grow as expected. For instance, at 600℃, the shape of the nanoparticles is cubic in nature. The TEM images

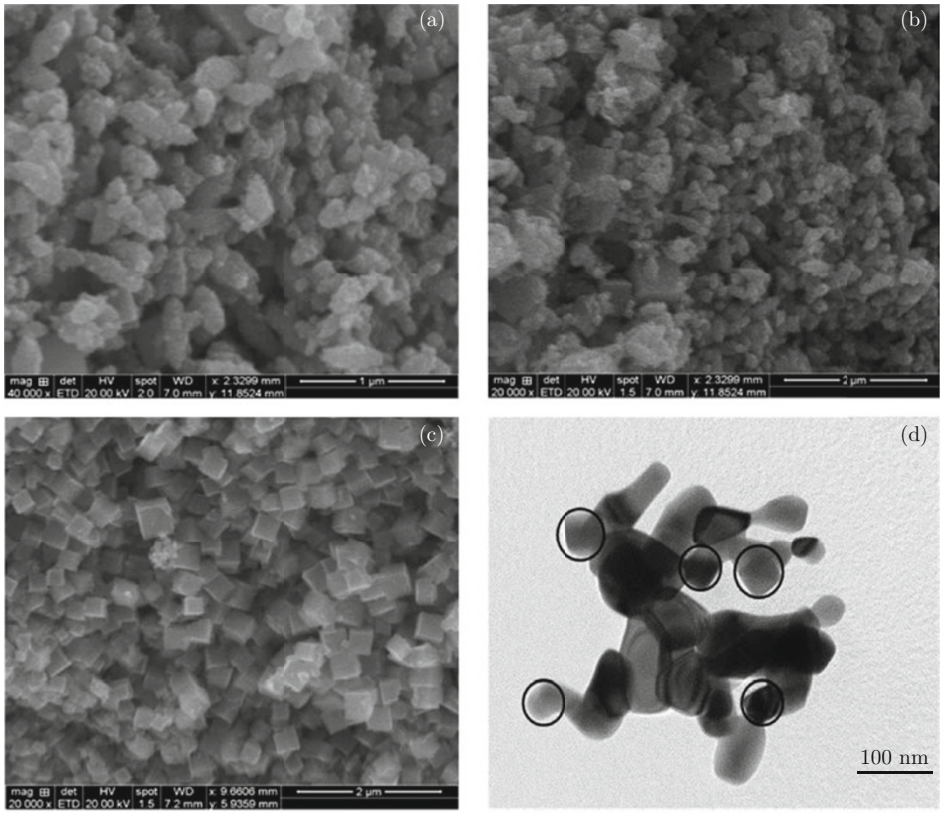

Fig. 3 SEM images of (a) ZTO precursor, (b) calcined at 300℃, (c) calcined at 600℃. (d) TEM image of ZTO calcined at 600℃.

of ZTO nanoparticles obtained from the electrolyte concentration of 30 mM $NaHCO_3$, 10 mM Na_2SnO_3 at 1 A/dm^2 and calcined at 600℃ for 1 hr are given in Fig. 3(d). It can be observed that ZTO nanoparticles are present as granules with clear cubic like shapes and are crystalline in nature. The average particles size ranges from 40-50 nm, which are in good agreement with the values calculated from XRD data by Debye-Scherrer equation.

FT-IR spectroscopy

Infrared spectroscopy was used to detect the presence of functional groups adsorbed on the surface of synthesized nanoparticles during electrochemical process. Figure 4 represents the FT-IR spectra of $Zn{\cdot}Sn(OH)_6$ and ZTO powder obtained from the bath concentration of 30 mM $NaHCO_3$, 10 mM Na_2SnO_3 at the current density of 1 A/dm^2. The as-prepared sample was heat-treated at different temperatures of 300, and 600℃ for 1 hr. Figure 4(a) indicates a strong and broad absorption peaks in the range of 3100-3600 cm^{-1} centered at 3447 cm^{-1}, corresponding to the stretching vibration of hydrogen bond (O-H) of surface adsorbed crystalline water and higher amount of hydroxyl group. These vibrations are the evidence for the existence of water in the as-prepared compound. These peaks gradually disappear under increasing calcinations temperature, indicating the removal of water. It is interesting to note that the two bands centered at 1652 and 1522 cm^{-1} are ascribed to the vibration of absorptive water. The weak band at 1040 cm^{-1} appearing in IR spectrum of as-prepared compound may be attributed to the vibrations of M-OH or M-OH-M groups for $Zn{\cdot}Sn(OH)_6$, and the absorption peak at 502 cm^{-1} is due to the vibration of M-O or M-O-M groups for ZTO nanoparticles. This indicates the presence of ZTO nanoparticles in as-prepared and calcined compounds. The metal oxygen's frequencies observed for the respective metal oxides are in accordance with literature's values for $Zn{\cdot}Sn(OH)_6$ and ZTO [40].

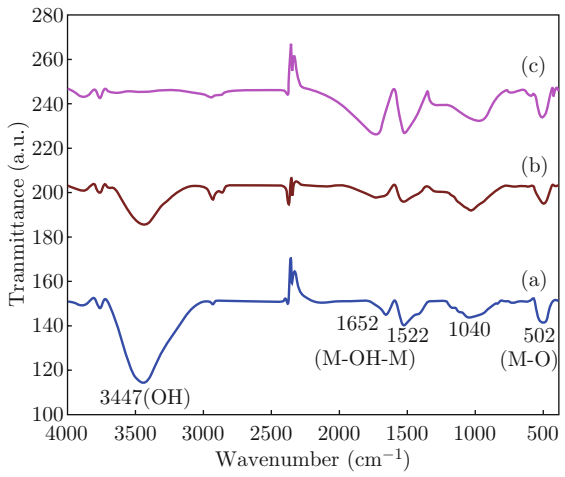

Fig. 4 FT-IR spectra of (a) ZTO precursorm, (b) calcined at 300℃ and (c) calcined at 600℃.

Evaluation of Photocatalytic Activity

Photocatalytic performance of ZTO with MB dye

The successful synthesis of ZTO nanoparticles offers an opportunity to examine their photocatalytic activity. The as-prepared and calcined ZTO nanoparticles were selected for the evaluation of photocatalytic activity with MB dye under the illumination of UV light. In order to study the effect of UV light on degradation of MB dye, a blank experiment was performed under UV light without the addition of photocatalysts (ZTO). The results indicated that MB dye of 10 mg/l was photolyzed up to 5% in 2 hr. This degradation efficiency was negligible when the different sized (24, 35 and 53 nm) nanoparticles were added to the solution under illumination. When there was no UV light, the concentration of MB dye with the addition of ZTO photocatalysts remains unchanged for 2 hr. From these blank experiments, it can be concluded that UV light and photocatalysts are the necessary factors in the photocatalytic process. The chemical structure of MB dye is shown in Fig. 5. MB dye absorbs light in the visible region (550-700 nm) with the absorption maxima at 664 nm. A series of experiments were carried out with different sizes (24, 35 and 53 nm) ZTO nanoparticles in

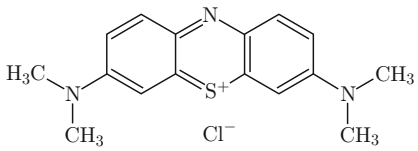

Fig. 5 Schematic of MB molecular structure.

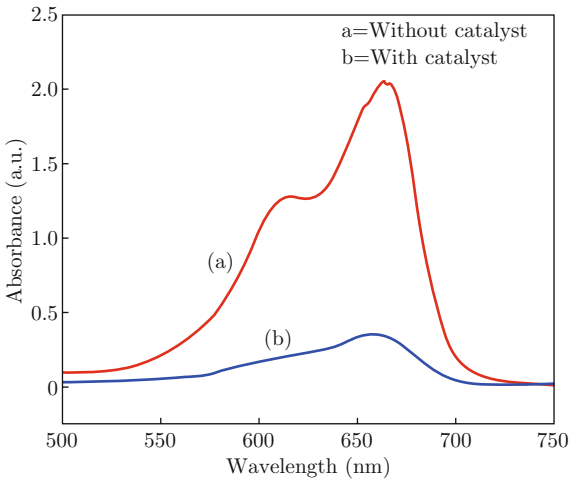

Fig. 6 UV-Vis absorption spectra of MB dye solution (a) without ZTO catalyst and (b) with ZTO catalyst.

MB dye solution. The UV-Visible spectra of MB dye (10 mg/l) solution without and with ZTO photocatalysts are shown in Fig. 6. It can be seen that the intensity of absorption peak corresponding to MB molecules at 664 nm decreases and blue-shifted towards 658 nm. This small hypsochromic shift indicates that the photodegradation of MB dye under UV light irradiation experiences a continuous removal of methyl groups. The percentage of decolorization and photodegradation increases with irradiation time.

Influence of calcination temperature on ZTO photocatalysts

The calcination temperature decided particle size (Table 1) and BET surface area affect the photocatalytic efficiency of nano ZTO. The particle size will increase with improved calcination temperature and decreased surface area, accompanied by a drop in photocatalytic activity. This suggests that the morphology of nano ZTO also plays a very important role in deciding the catalyst performance. The degradation efficiencies of different sized ZTO photocatalysts compared with commercially available TiO_2 on MB dye solution are shown in Fig. 7. It can be observed from Fig. 7(a) that there is a small degradation with the as-prepared ZTO nanoparticles. In the initial 60 min, the degradation efficiency reached the highest value of 40%. Afterward, the degradation efficiency ascends tardily up to the maximum of 50%. Figure 7(b) shows the time-dependent UV-Visible spectra of MB dye solution containing calcined (300℃) ZTO nanoparticles. The efficiency of degradation is somewhat higher compared with the as-prepared sample which reaches the highest value of 70%. But in the sample calcined at 600℃ (Fig. 7(c)), there is a large degradation observed. In the initial 20 min, the degradation efficiency reached the highest value of 60%. Afterward, the absorbance curve decreases and the efficiency of degradation ascend tardily up to almost 90%. The crucial degradation efficiency after 80 min illumination has changed a little

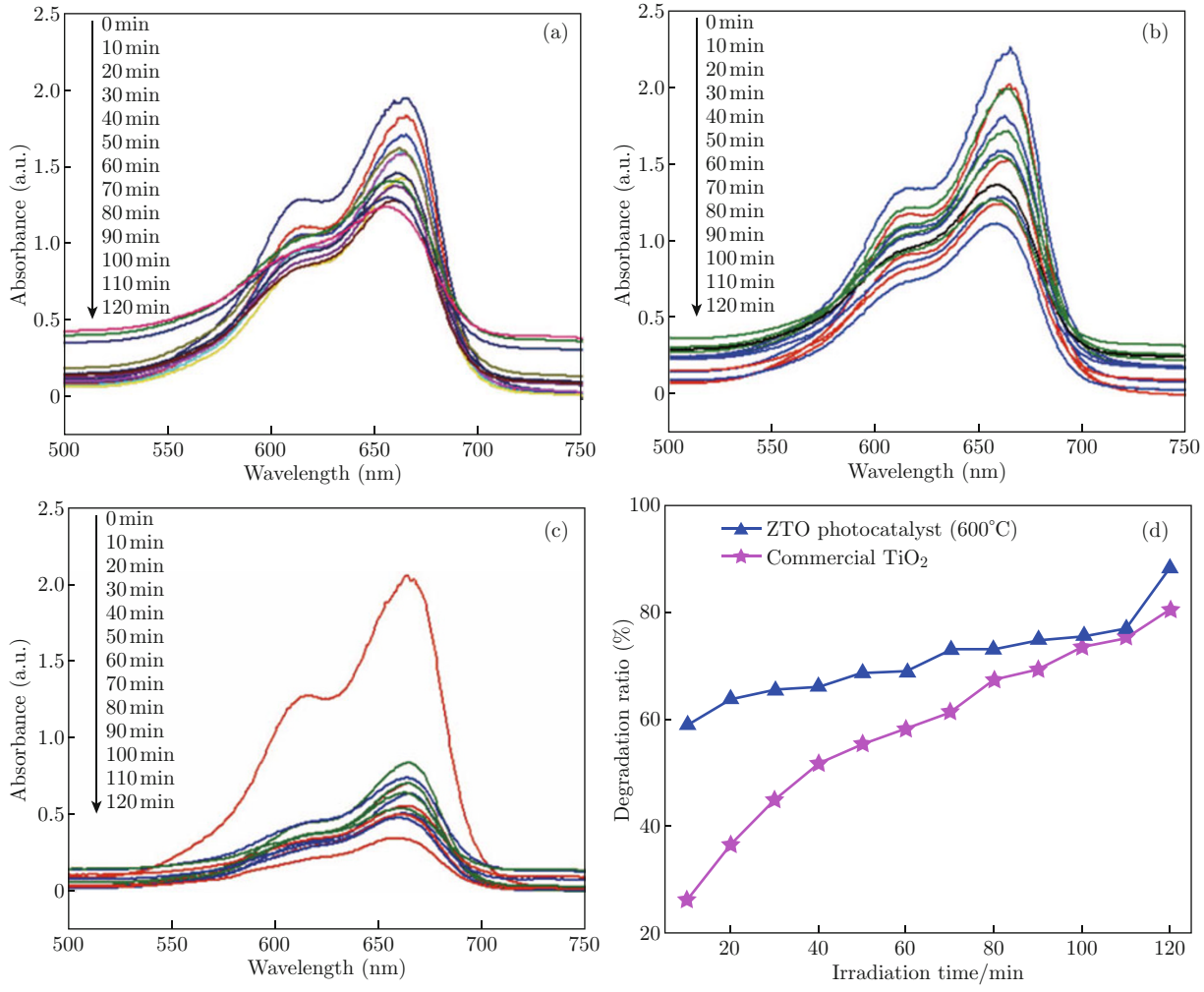

Fig. 7 Time-dependent absorption spectra of MB dye during UV light irradiation in presence of ZTO (a) as-prepared, (b) calcined at 300℃, (c) calcined at 600℃ and (d) degradation rate of two different catalysts.

compared with the efficiency obtained after the initial illumination for 20 min. The relative bigger size and the reduction of the number of surface hydroxyl are the main reasons for the decrease of degradation efficiency of photocatalysts [37]. The increase of particle size with increased calcination temperature to 600℃ (Fig. 7(c)) is helpful to increase the photocatalytic activity. However, a higher catalytic activity is observed for calcined ZTO sample only in the early stage of reaction (30 min), the percentage of activity is little increased for longer time degradation.

Evaluation of photodegradation

The catalytic activity of ZTO photocatalysts was evaluated by MB dye in aqueous solution and it was compared with that of commercially available TiO_2-P25 photocatalysts. Figure 7(d) shows the degradation ratio of calcined (600℃) ZTO photocatalysts compared with that of commercially available TiO_2-P25 photocatalysts, which was evaluated by the degradation of MB dye in aqueous solution. The performance of degradation process was defined as % Degradation = $(A_o - A)/A_o \times 100\%$, where A_o is the initial absorbance and A is the final absorbance. The degradation of dye molecules by self-direct photolysis was negligible. The activity of ZTO photocatalysts is slightly greater but it is almost equal to commercial TiO_2-P25 photocatalysts, which is attributed to its high surface area (41.8 m^2/g), higher crystallinity and smaller particle size ($\approx$ 19 nm). The catalytic performance on degradation is a complex function involving several parameters such as morphology, charge density, dye adsorption capacity, and is related to the BET surface area and pore size distribution. Lou *et al.* [11] observed that ZTO nanocrystals exhibited high photocatalytic activity to various reactive dyes such as K-NR, B-RN and B-GFF because of their large surface area ($\approx$ 62 m^2/g). Zhang *et al.* [25] observed that oxide coupled ZnO-SnO_2 nanocrystals had equally excellent photocatalytic activity for the degradation of methyl orange when compared to TiO_2-P25. The degradation efficiency of ZTO nanoparticles calcined at different temperature reduced in the order of 600℃ > 300℃ > 60℃.

Enhancement of UV activity

In photocatalytic mechanism, the main oxidative groups (radicals, holes and O_2^-) could be detected through trapping experiments of respective scavengers. Large number of enhancement is mainly due to high charge separation induced by surface oxygen-vacancies states. It is advantageous to increase the transport rate of photogeneration carriers, for the improved charge separation efficiency and diminished probability of photogenerated electron-hole pairs' recombination. This leads to an improved photocatalytic activity. A proposed schematic for electron-hole separation together with the energy level diagram for ZTO photocatalysts and TiO_2 is shown in Fig. 8. The above results recommend that the photogenerated holes are the main oxidative centers of ZTO system. This suggests that calcined ZTO nanoparticles are highly efficient photocatalysts when compared to commercially available TiO_2-P25 photocatalysts for the degradation of MB dye.

Conclusions

In the present work, the nanosized ZTO particles were successfully synthesized by hybrid electrochemical-thermal method using $NaHCO_3$ and Na_2SnO_3 electrolyte, without zinc salts, templates or surfactants. The generated Zn^{2+} ions at Zn electrode combined with Sn^{2+} ions from sodium stannate were

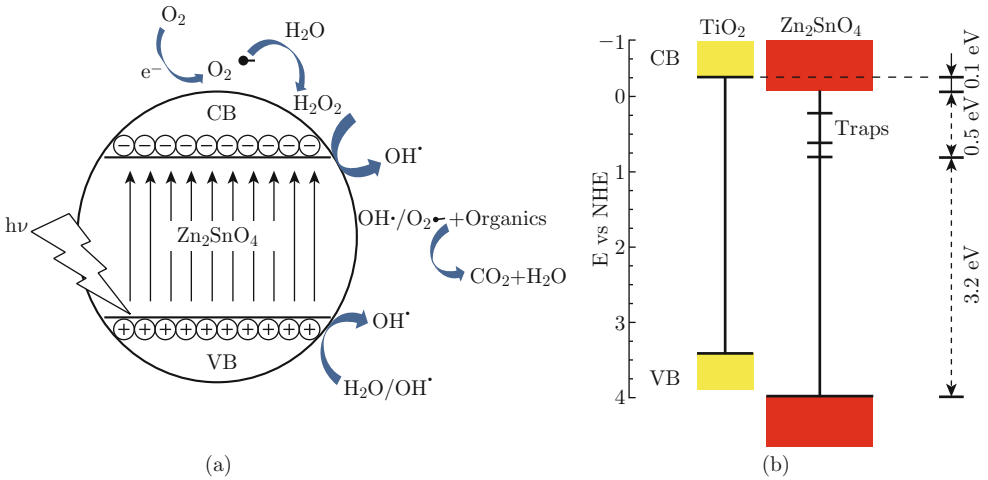

Fig. 8 Illustration of the charge separation mechanism (a) photocatalytic reaction process of ZTO photocatalysts under UV light. (b) Energy level diagram of TiO_2 (E_g = 3.2 eV) and Zn_2SnO_4 (E_g = 3.7 eV) photocatalysts.

converted into ZTO during electrolysis. The particle size range of the generated ZTO powder was 24-53 nm. The FT-IR spectrum shows the existence of OH^-, M-OH-M and M-O-M groups in uncalcined sample. After calcinations, the particles morphology was cubic like and is well crystallized in the nanosize of 40-50 on nanometer scale. The method could be effectively used to synthesize ZTO on large scale. Also, the evaluations of photocatalytic degradation of MB dye with different sizes ZTO photocatalysts were preformed and compared with commercially available TiO_2-P25. The as-prepared ZTO exhibited an efficient catalytic activity in degrading MB dye, and the calcined ZTO has higher photocatalytic activity compared to TiO_2-P25 under UV light irradiation. The higher photocatalytic property was probably caused by larger crystallanity and smaller particle size. Thus, synthesized by the simple, fast and eco-friendly electrochemical method, the nano ZTO is a promising candidate for the photodegradation of dyes from wastewaters.

Acknowledgements

The authors gratefully acknowledge the Kuvempu University in India and NANOCAT research centre of University of Malaya in Malaysia for providing the lab facilities to bring about this work. One of the authors KGC thanks CSIR of New-Delhi of Government of India (GOI) for SRF [Sanction No. 09/908(0002) 2K9-EMR-I] during 2009-2012.

References

[1] Y. K. Park, E. H. Tadd, M. Zubris and R. Tannenbaum, "Size-controlled synthesis of Alumina nanoparticles from aluminum alkoxides", Mater. Res. Bull. 40(9), 1506-1512 (2005). http://dx.doi.org/10.1016/j.materresbull.2005.04.031

[2] M. R. Hoffmann, S. T. Martin, W. Y. Choi and D. W. Bahnemann, "Environmental applications of semiconductor Photocatalysis", Chem. Rev. 95(1), 69-96 (1995). http://dx.doi.org/10.1021/cr00033a004

[3] T. Sehili, P. Boule and J. Lemaire, "Photocatalysed transformation of chloroaromatic derivatives on zinc oxide II-dichlorobenzenes", J. Photochem. Photobio. A: Chem. 50(1), 103-116 (1989). http://dx.doi.org/10.1016/1010-6030(89)80024-3

[4] J. Villasenor, P. Reyes and G. Pecchi, "Photodegradation of pentachlorophenol on ZnO", J. Chem. Tech. Biotech. 72(2), 105-110 (1998). http://dx.doi.org/10.1002/(SICI)1097-4660(199806)72:2<105::AID-JCTB883>3.3.CO;2-S

[5] M. D. Driessen, T. M. Miller and V. H. Grassian, "Photocatalytic oxidation of trichloroethylene on zinc oxide: characterization of surface-bound and gas-phase products and intermediates with FT-IR spectroscopy", J. Mol. Catal A: Chem. 131(1-3), 149-156 (1998). http://dx.doi.org/10.1016/S1381-1169(97)00262-8

[6] B. Tan, E. Toman, Y. G. Li and Y. Y. Wu, "Zinc stannate (Zn_2SnO_4) dye-sensitized solar cells", J. Am. Chem. Soc. 129(14), 4162-4163 (2007). http://dx.doi.org/10.1021/ja070804f

[7] I. Stambolova, K. Konstantinov, D. Kovacheva, P. Peshev and T. Donchev, "Spray pyrolysis preparation and humidity sensing characteristics of spinel zinc stannate thin films", J. Solid State Chem. 128(2), 305-309 (1997). http://dx.doi.org/10.1006/jssc.1996.7174

[8] J. H. Yu and G. M. Choi, "Current-voltage characteristics and selective CO detection of Zn_2SnO_4 and ZnO/Zn_2SnO_4, SnO_2/Zn_2SnO_4 layered-type sensors", Sens. Actuator B 72(2), 141-148 (2001). http://dx.doi.org/10.1016/S0925-4005(00)00642-0

[9] F. Belliard, P. A. Connor and J. T. S. Irvine, "Novel tin oxide-based anodes for Li-ion batteries", Solid State Ionics. 135(1-4), 163-167 (2000). http://dx.doi.org/10.1016/S0167-2738(00)00296-4

[10] A. Rong, X. P. Gao, G. R. Li, T. Y. Yan, H. Y. Zhu, J. Q. Qu and D. Y. Song, "Hydrothermal synthesis of Zn_2SnO_4 as anode materials for Li-ion battery", J. Phys. Chem. B 110(30), 14754-14760 (2006). http://dx.doi.org/10.1021/jp062875r

[11] X. D. Lou, X. H. Jia, J. Q. Xu, S. Z. Liu and Q. H. Gao, "Hydrothermal synthesis, characterization and photocatalytic properties of Zn_2SnO_4 nanocrystal", Mater. Sci. Eng. A 432(1-2), 221-225 (2006). http://dx.doi.org/10.1016/j.msea.2006.06.010

[12] W. Cun, X. M. Wang, J. C. Zhao, B. X. Mai, G. Y. Sheng, P. A. Peng and J. M. Fu, "Synthesis, characterization and photocatalytic property of nano-sized Zn_2SnO_4", J. Mater. Sci. 37(14), 2989-2996 (2002). http://dx.doi.org/10.1023/A:1016077216172

[13] S. Wang, Z. Yang, M. Lu, Y. Zhou, G. Zhou, Z. Qiu, S. Wang, H. Zhang and A. Zhang, "Coprecipitation synthesis of hollow Zn_2SnO_4 spheres", Mater. Lett. 61, 3005-3008 (2007). http://dx.doi.org/10.1016/j.matlet.2006.07.197

[14] E. L. Foletto, S. L. Jahn and R. F. P. M. Moreira, "Hydrothermal preparation of Zn_2SnO_4 nanocrystals and photocatalytic degradation of a leather dye", J. Appl. Electrochem. 40(14-15), 59-63 (2010). http://dx.doi.org/10.1007/s10800-009-9967-2

[15] X. Fu, X. Wang, J. Jong, Z. Ding, T.Yan, G. Zhang, Z. Zhang, H. Lin and X. Z. Fu, "Hydrothermal synthesis, characterization, and photocatalytic properties of Zn_2SnO_4", J. Solid State Chem. 182(3), 517-524 (2009). http://dx.doi.org/10.1016/j.jssc.2008.11.029

[16] J. Zeng, M. D. Xin, K. W. Li, H. Wang, H. Yan and W. J. Zhang, "Transformation process and photocatalytic activities of hydrothermally synthesized Zn_2SnO_4

nanocrystals", J. Phys. Chem. C 112(11), 4159-4167 (2008). http://dx.doi.org/10.1021/jp7113797

[17] Y. Lin, S. Lin, M. Luo and J. Liu, "Enhanced visible light photocatalytic activity of Zn_2SnO_4 via sulfur anion-doping", Mater. Lett. 63(13-14), 1169-1171 (2009). http://dx.doi.org/10.1016/j.matlet.2009.02.020

[18] Yu Shiang Wu, Wen Ku Chang and Min Jou, "Photocatalytic analysis and characterization of Zn_2SnO_4 nanoparticles synthesized via hydrothermal method with Na_2CO_3 mineralizer", Adv. Mater. Res. 97, 19-22 (2010). http://dx.doi.org/10.4028/www.scientific.net/AMR.97-101.19

[19] A. A. Firooz, A. R. Mahjouba, A. A. Khodadadi and M. Movahedi, "High photocatalytic activity of Zn_2SnO_4 among various nanostructures of $Zn_{2x}Sn_{1-x}O_2$ prepared by a hydrothermal method", Chem. Eng. J. 165(2), 735-739 (2010). http://dx.doi.org/10.1016/j.cej.2010.09.052

[20] Z. Ai, S. Lee, Y. Huang, W. Ho and L. Zhang, "Photocatalytic removal of NO and HCHO over nanocrystalline Zn_2SnO_4 microcubes for indoor air purification", J. Hazard. Mater. 179(1-3), 141-150 (2010). http://dx.doi.org/10.1016/j.jhazmat.2010.02.071

[21] M. J. Kim, S. H. Park and Y. D. Huh, "Photocatalytic activities of hydrothermally synthesized Zn_2SnO_4", Bull. Korean Chem. Soc. 32(5), 1757-1760 (2011). http://dx.doi.org/10.5012/bkcs.2011.32.5.1757

[22] E. L. Foletto, J. M. Simoes, M. A. Mazutti, S. L. Jahn, E. I. Muller, L. S. F. Pereirab and E. M. M. Floresb, "Application of Zn_2SnO_4 photocatalyst prepared by microwave-assisted hydrothermal route in the degradation of organic pollutant under sunlight", Ceramics Inter. 39(4), 4569-4574 (2013). http://dx.doi.org/10.1016/j.ceramint.2012.11.053

[23] H. Y. Chen, J. X. Wang, H. C. Yu, H. X. Yang, S. S. Xie and J. Q. Li, "Transmission electron microscopy study of pseudo periodically twinned Zn_2SnO_4 nanowires", J. Phys. Chem. B 109(7), 2573-2577 (2005). http://dx.doi.org/10.1021/jp046125y

[24] J. S. Jie, G. Z. Wang, X. H. Han, J. P. Fang, Q. X. Yu, Y. Liao, B. Xu, Q. T. Wang and J. G. Hou, "Growth of ternary oxide nanowires by gold-catalyzed vapor-phase evaporation", J. Phys. Chem. B 108(24), 8249-8253 (2004). http://dx.doi.org/10.1021/jp049230g

[25] M. Zhang, T. An, X. Hu, C. Wang, G. Sheng and J. Fu, "Preparation and photocatalytic properties of a nanometer ZnO-SnO_2 coupled oxide", Appl. Catal. A: Gen 260(2), 215-222 (2004). http://dx.doi.org/10.1016/j.apcata.2003.10.025

[26] G. Fu, H. Chen, Z. X. Chen, J. X. Zhang and H. Kohler, "Humidity sensing characteristics of Zn_2SnO_4-$LiZnVO_4$ thick films prepared by the sol-gel method", Sens. Actuator B 81(2-3), 308-312 (2002). http://dx.doi.org/10.1016/S0925-4005(01)00971-6

[27] A. Kurz, K. Brakecha, J. Puetz and M. A. Aegerter, "Strategies for novel transparent conducting sol-gel oxide coatings", Thin Solid Films 502(1-2), 212-218 (2006). http://dx.doi.org/10.1016/j.tsf.2005.07.276

[28] N. Nikolic, Z. Marinkovic and T. Sreckovic, "The influence of grinding conditions on the mechanochemical synthesis of zinc stannate", J. Mater. Sci. 39(16-17), 5239-5242 (2004). http://dx.doi.org/10.1023/B:JMSC.0000039218.82254.a4

[29] H. L. Zhu, D. R. Yang, G. X. Yu, H. Zhang, D. L. Jin and K. H. Yao, "Hydrothermal synthesis of Zn_2SnO_4 nanorods in the diameter regime of sub-5 nm and their properties", J. Phys. Chem. B 110(15), 7631-7634 (2006). http://dx.doi.org/10.1021/jp060304t

[30] J. Fang, A. H. Huang, P. X. Zhu, N. S. Xu, J. Q. Xie, J. S. Chi, S. H. Feng, R. R. Xu and M. M. Wu, "Hydrothermal preparation and characterization of Zn_2SnO_4 particles", Mater. Res. Bull. 36(7-8), 1391-1397 (2001). http://dx.doi.org/10.1016/S0025-5408(01)00621-3

[31] J. Zeng, M. D. Xin, K. W. Li, H. Wang, H. Yan and W. J. Zhang, "Transformation process and photocatalytic activities of hydrothermally synthesized Zn_2SnO_4 nanocrystals", J. Phys. Chem. C 112(11), 4159-4167 (2008). http://dx.doi.org/10.1021/jp7113797

[32] E. Boschke, U. Bohmer, J. Lange, M. Constapel, M. Schellentrager and T. Bley, "The use of respirometric measurements to determine the toxicity of textile dyes in aqueous solution and after oxidative decolourisation processes", Chemosphere. 67(11), 2163-2168 (2007). http://dx.doi.org/10.1016/j.chemosphere.2006.12.041

[33] H. Wang, C. Xie, W. Zhang, S. Cai, Z. Yang and Y. Gui, "Comparison of dye degradation efficiency using ZnO powders with various size scales", J. Hazard. Mater. 141(3), 645-652 (2007). http://dx.doi.org/10.1016/j.jhazmat.2006.07.021

[34] R. Y. Hong, J. H. Li, L. L. Chen, D. Q. Liu, H. Z. Li, Y. Zheng and J. Ding, "Synthesis, surface modification and photocatalytic property of ZnO nanoparticles", Powder Technology. 189(3), 426-432 (2009). http://dx.doi.org/10.1016/j.powtec.2008.07.004

[35] R. M. Trommer, A. K. Alves and C. P. Bergmann, "Synthesis, characterization and photocatalytic property of flame sprayed zinc oxide nanoparticles", J. Alloys Compd. 491(1-2), 296-300 (2010). http://dx.doi.org/10.1016/j.jallcom.2009.10.147

[36] X. Ren, D. Han, D. Chen and F. Tang, "Large-scale synthesis of hexagonal cone-shaped ZnO nanoparticles with a simple route and their application to photocatalytic degradation", Mater. Res. Bull. 42(5), 807-813 (2007). http://dx.doi.org/10.1016/j.materresbull.2006.08.030

[37] K. G. Chandrappa and T. V. Venkatesha, "Electrochemical Synthesis and photocatalytic property of zinc oxide nanoparticles", Nano-Micro Lett. 4(1), 14-24 (2012). http://dx.doi.org/110.3786/nml.v4i1.p14-24

[38] K. G. Chandrappa, T. V. Venkatesha, K. Vathsala and C. Shivakumara, "A hybrid electrochemical-thermal method for the preparation of large ZnO nanoparticles", J. Nanopart. Res. 12(7), 2667-2678 (2010). http://dx.doi.org/10.1007/s11051-009-9846-0

[39] P. Scherrer, Nachr. Ges. Wiss. Goettingen, Mathematical Physics K_l 26, 98-100 (1918).

[40] C. N. R. Rao, "Chemical Applications of Infrared Spectroscopy", Academic Press, New York-London (1963).